GSA Data Repository 2019204

Young, N.E. *et al.,* Early Younger Dryas glacier culmination in southern Alaska: Implications for North Atlantic climate change during the last deglaciation.

Figure S1: Aerial view of Mt. Waskey moraines

Figure S2: Field photographs of representative sampled boulders

Figure S3: ^{10}Be probability density estimates for the sampled Mt. Waskey moraines

Table S1: Mt. Waskey ^{10}Be sample information

Table S2: Process blank ^{10}Be data

Materials and Methods

Geochemistry and AMS analysis

All samples from the Waskey Lake region, Ahklun Mountains, southwestern Alaska were processed at the Lamont-Doherty Earth Observatory (LDEO) cosmogenic dating laboratory (n = 19; Table S1). Quartz separation and Be isolation followed well established protocols (Schaefer et al., 2009) and accelerator mass spectrometric (AMS) analyses were completed at the Center for Accelerator Mass Spectrometry at Lawrence Livermore National Laboratory and measured relative to the 07KNSTD standard with ^{10}Be/^{9}Be ratio of 2.85 x 10^{-12} (Nishiizumi et al., 2007). The 1σ analytical error ranged from 1.7% to 3.2%, with a mean of 2.1 ± 0.4% (Table S1). Process blank corrections were applied by taking the batch-specific blank value (expressed as # of ^{10}Be atoms) and subtracting this value from the sample ^{10}Be atom count; individual blank measurements ranged from 1925 ± 801 to 4375 ± 1116 ^{10}Be atoms (n=4; Table S2).

^{10}Be sampling and age calculations

The Mt. Waskey moraines are, notably, clast-supported, which encourages exceptional moraine stability because significant moraine degradation is unlikely to occur in a clast-supported setting versus a moraine dominated by fine-grained matrix. Alaska is a particularly active geomorphic environment (e.g. seasonal freeze-thaw) which, historically, has complicated the use of ^{10}Be dating in the region (Briner et al., 2005). Thus, the relative stability of the Mt. Waskey moraines offers an opportunity to develop a high-resolution ^{10}Be based chronology of glacier change in a setting where boulder exhumation, which results in ^{10}Be ages that underestimate the true age of moraine deposition, is likely minimal to non-existent. When sampling, we capitalized on this stability by only sampling the clast-supported left-lateral moraines (Figs. S1 and S2), while choosing not to sample the end or right-lateral moraine segments that are not clast-supported. The left-lateral segments of the Mt. Waskey moraines rest directly down flow line from a section of the valley wall that is near vertical and displays obvious signs of extensive boulder quarrying. This segment of the valley wall most likely acts as the primary source region for the abundance of boulders that comprise the left-lateral segments of the Mt. Waskey moraines. For reference, see the topography displayed in Fig. 1B, and the upper right corner of the photograph for sample 14AK-27 (Fig. S2).

Samples from granodioritic boulders were collected using a Hilti brand AG500-A18 angle grinder/circular saw and a hammer and chisel. Sample locations and elevation were collected with a handheld GPS unit with a vertical uncertainty of $\pm$5 m. A handheld clinometer was used to measure topographic shielding by the surrounding topography.

^{10}Be surface exposure ages were calculated using the Baffin Bay ^{10}Be production-rate calibration dataset (Young et al., 2013), and 'Lm' scaling (Lal, 1991; Stone, 2000) as the effects of changes in the geomagnetic field are minimal at this high latitude. The Baffin Bay production rate benefits from three independent and statistically identical calibration datasets that are combined into one calibration dataset. The Baffin Bay Baffin Bay ^{10}Be production rate is statistically identical to other Northern Hemisphere high-latitude ^{10}Be calibration sites with well-constrained independent chronologies such as the northeastern North America and Rannoch Moor, Scottish Highlands, reference production rates (Balco et al., 2009; Putnam et al., 2019). Ages are calculated using version 3 of the exposure age calculator found at https://hess.ess.washington.edu/, that implements an updated treatment of muon-based nuclide production (Balco et al., 2008; Balco, 2017). We do not correct measured nuclide concentrations for the effects of snow-cover or surface erosion; samples are almost exclusively from windswept locations and many surfaces still retained primary glacial features. Individual ^{10}Be ages are presented and discussed with 1-sigma analytical uncertainties only, and when moraine ages are compared to independent records, the production rate uncertainty is propagated through in quadrature (Fig. 2; Fig, 3; Table S1).

Original vs. new ^{10}Be measurements

Re-dating of the Mt. Waskey moraines provides are unique opportunity to compare two generations of ^{10}Be measurements from the same geological features. Furthermore, although ^{10}Be extraction occurred in different laboratories, both generations of ^{10}Be measurements were made at LLNL-CAMS. Briner et al., 2002 presented 7 ^{10}Be measurements from the Mt. Waskey moraines: 4 measurements from boulders resting on the terminal moraine (M1), 2 measurements from boulders resting on M3, and lastly, a single measurement from a moraine boulder resting on a Waskey equivalent moraine in a small valley ~2 km west of the main Waskey Lake field area (Table S1). After disregarding two older outliers, which likely contain isotopic inheritance (MB1-99-2: 16.58 $\pm$ 1.73 ka and MB1-99-3: 17.17 $\pm$ 2.27 ka; Table S1), the remaining ^{10}Be ages from the M1 terminal moraine are 11.97 $\pm$ 2.06 ka and 11.57 $\pm$ 0.65 ka. In comparison, ^{10}Be ages from M1 presented in this study have a mean value of 12.52 $\pm$ 0.07 (n=7; Table S1). These two generations of ^{10}Be measurements from M1 contain a single replicate analysis: samples MB1-00-4 (Briner et al. 2002; 11.57 $\pm$ 0.65 ka) and 14AK-09 (this study; 12.60 $\pm$ 0.27 ka) are from the same moraine boulder, albeit two different sample collections (Table S1; Figure S2). These two measurements do not overlap a 1σ analytical uncertainty and we did not note any reason in field why our two sample collections from the same boulder would yield noticeably different ^{10}Be ages – samples were collected from the same general upper region of the boulder surface with no obvious signs of preferential erosion at the original sample location. In addition, Briner et al., 2002 presented two ages from M3 of 11.90 $\pm$ 0.50 ka and 10.44 $\pm$ 0.67 ka, compared to a mean value of 12.09 $\pm$ 0.44 ka presented here (n=6; Table S1).

Whereas the total number of measurements combined with the measurement precision in our new ^{10}Be dataset presented here allow us to chronologically distinguish between distinct morphostratigraphic features (M1 vs. M3 vs. inboard of M3), all ^{10}Be ages, regardless of feature, overlap in the original Briner et al. 2002 dataset (Table S1). Combining all of the original ^{10}Be measurements in one population results in a mean age 11.31 $\pm$ 0.71 ka (n=5), compared to a value of 12.32 $\pm$ 0.36 (n=13) for the re-measurements. While these values narrowly overlap at 1σ, these values, combined with the replicate analysis are suggestive of our new ^{10}Be ages being systematically older than the Briner et al., 2002 ^{10}Be ages despite being calculated with the same methods (Table S1). This offset can almost certainly not be explained by field sampling strategies. Systematically younger ages in original dataset would require a scenario where Briner et al., 2002 sampled 1) only boulders with that had undergone a slight amount of exhumation relative to the 2014 field season samples, or 2) portions of boulder surfaces that had undergone a slight amount of preferential erosion compared to all the sampled surfaces in the 2014 field season; neither of these scenarios seem likely. Instead, we suspect it is possible that the stated concentration for the ^{9}Be carrier used in the Briner et al., (2002) measurements (1000 ppm) was ~5-8% less than the true concentration via either evaporative enrichment or a slightly erroneous initial measurement of the carrier concentration.

References

Balco, G., 2017, Production rate calculations for cosmic-ray-muon-produced ^{10}Be and ^{26}Al benchmarked against geological calibration data: Quaternary Geochronology, v. 39, p. 150-173.

Balco, G., Stone, J., Lifton, N., and Dunai, T.J., 2008, A simple, internally consistent, and easily accessible means of calculating surface exposure ages and erosion rates from Be-10 and Al-26 measurements. Quaternary Geochronology, v. 3, p. 174–195.

Balco, G., Briner, J.P., Finkel. R.C., Rayburn, J.A., Ridge, J.C., and Schaefer, J.M., 2009, Regional beryllium-10 production rate calibration for late-glacial northeastern North America: Quaternary Geochronology, v. 4, p. 93-107.

Briner, J.P., Kaufman, D.S., Manley, W.F., Finkel, R.C., Caffee, M.W., 2005, Cosmogenic exposure dating of late Pleistocene moraine stabilization in Alaska: GSA Bulletin, v. 117, p. 1108-1120.

Lal, D., 1991, Cosmic ray labeling of erosion surfaces: in situ nuclide production rates and erosion models: Earth and Planetary Science Letters, v. 104, 424-429.

Nishiizumi, K., Imamura, M., Caffee, M.W., Southon, J.R., Finkel, R.C., and McAninch, J., 2007, Absolute calibration of ^{10}Be AMS standards: Nuclear Instruments and Methods in Physics Research B, v. 258, p. 403-413.

Putnam, A.E., Bromley, G.R.M., Rademaker, K., and Schaefer, J.M., 2019, *In situ* ^{10}Be production-rate calibration from a ^{14}C-dated late-glacial moraine belt in Rannoch Moor, central Scottish Highlands: Quaternary Geochronology, v. 50, p. 109-125.

Schaefer, J.M., Denton, G.H., Kaplan, M., Putnam, A., Finkel, R.C., Barrell, D.J.A., Andersen, B.G., Schwartz, R., Mackintosh, A., Chinn, T., and Schlüchter, C., 2009, High-frequency Holocene glacier fluctuations in New Zealand differ from the Northern signature: Science, v. 324, p. 622-625.

Stone, J.O., 2000, Air pressure and cosmogenic isotope production: Journal of Geophysical Research, v. 105, p. 23,753-23,759

Young, N.E., Schaefer, J.M, Briner, J.P., and Goehring, B.M., 2013, A ^{10}Be production-rate calibration for the Arctic: Journal of Quaternary Science, v. 28, p. 515-526.

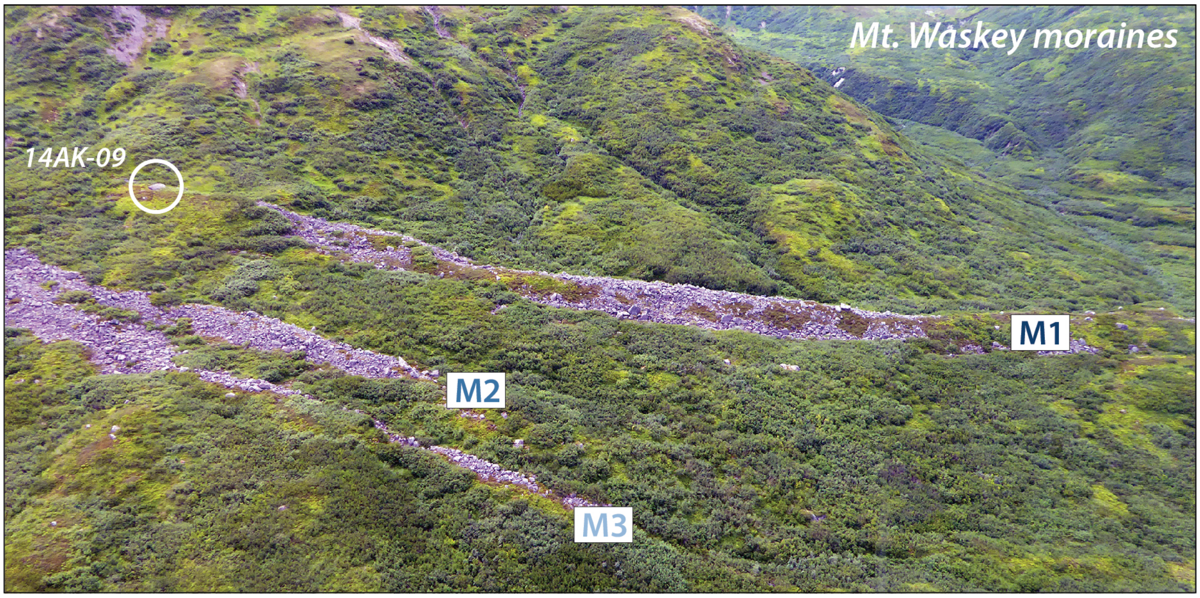

Figure S1. Aerial view of the Mt. Waskey moraines (left lateral).

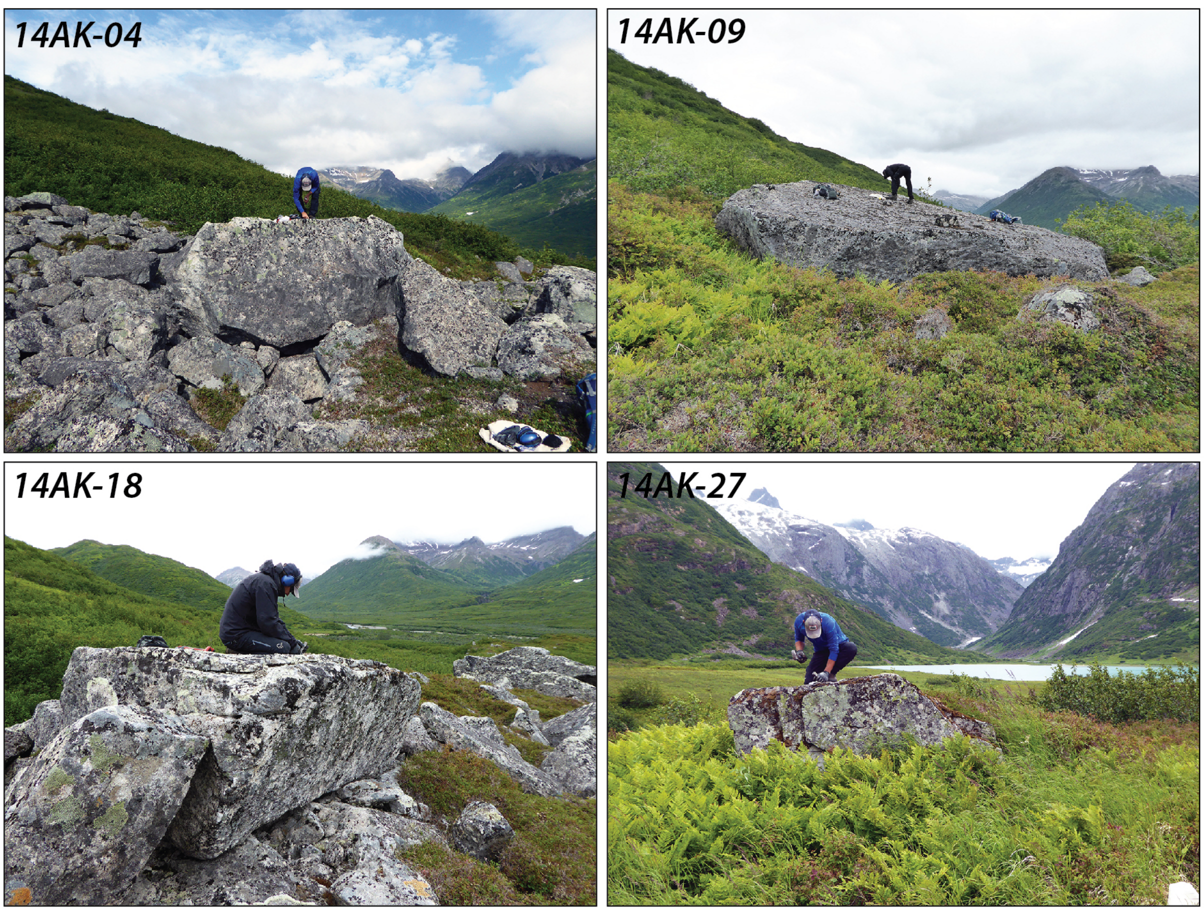

Figure S2. Representative boulders sampled in the field: 14AK-04 (M3; 12.04 ± 0.25 ka), 14AK-09 (M1; 12.60 ± 0.27 ka), 14AK-18 (M1; 12.58 ± 0.22 ka), and 14AK-27 (inboard erratic; 11.59 ± 0.30 ka). See Table S1 for details.

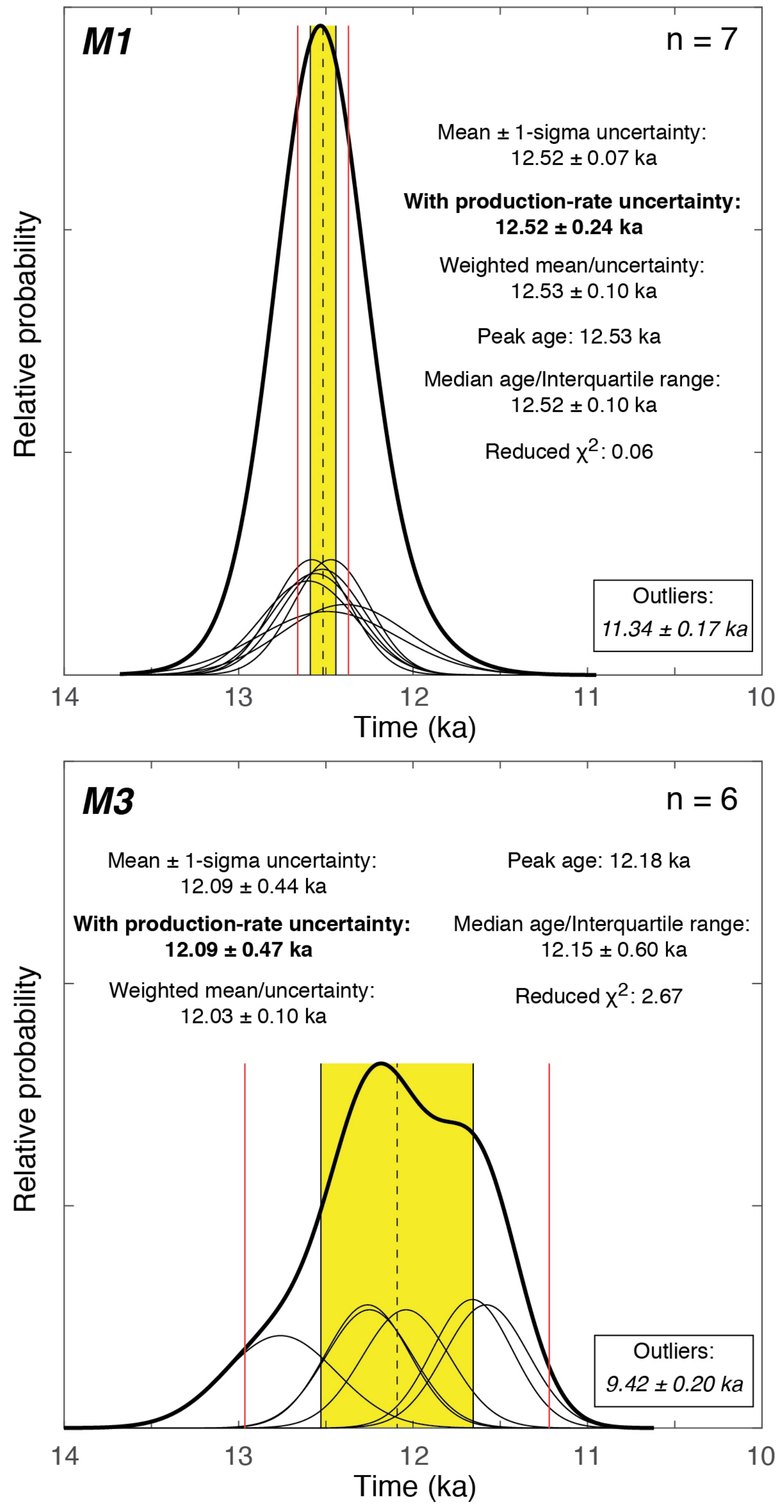

Figure S3. Probability density estimates and statistics for ^{10}Be ages from the outer (M1) and inner (M3) Mt. Waskey moraines (Table S1).

Table DR1. Mt. Waskey ^{10}Be sample information

Sample	Latitude	Longitude	Elevation (m asl)	Thickness (cm)	Shielding	Quartz (g)	Carrier added (g)[a]	^{10}Be/^{9}Be ratio (10^{-14})[b]	± 1σ Uncertainty (10^{-15})	Blank-corrected ^{10}Be concentration (atoms g^{-1})[c]	Blank-corrected ^{10}Be conc. uncertainty (atoms g^{-1})[c]	Age ka (Lm)	AMS Facility
Outer Waskey moraine - M1													
14AK-09	59.8676	-159.2196	287	1.53	0.988	15.0812	0.1811	8.0454	1.6997	71615	1526	12.60 ± 0.27	LLNL-CAMS
14AK-10	59.8683	-159.2204	273	2.53	0.988	27.8634	0.1821	13.9243	2.0554	63039	936	*11.34 ± 0.17*	LLNL-CAMS
14AK-12	59.8686	-159.2209	270	2.59	0.988	16.4703	0.1803	9.1080	1.5533	69024	1189	12.47 ± 0.22	LLNL-CAMS
14AK-15	59.8692	-159.2213	250	1.66	0.988	12.5264	0.1788	6.9189	2.1908	68289	2173	12.49 ± 0.40	LLNL-CAMS
14AK-16	59.8696	-159.2217	243	1.34	0.988	9.4042	0.1825	5.0849	1.0123	68335	1367	12.56 ± 0.25	LLNL-CAMS
14AK-17	59.8699	-159.2225	240	1.17	0.988	5.8526	0.1817	3.1425	8.8151	67307	1944	12.39 ± 0.36	LLNL-CAMS
14AK-18	59.8703	-159.2233	229	1.49	0.988	19.8353	0.1813	10.6490	1.8417	67411	1170	12.58 ± 0.22	LLNL-CAMS
14AK-19	59.8703	-159.2233	230	1.82	0.988	12.8396	0.1827	6.7925	1.3005	66983	1287	12.52 ± 0.24	LLNL-CAMS
											Mean ± 1 S.D.	**12.52 ± 0.07 (0.24)**	
Inner Waskey moraine - M3													
14AK-04	59.8669	-159.2179	287	1.76	0.988	15.6745	0.1811	8.5236	1.7687	68244	1420	12.04 ± 0.25	LLNL-CAMS
14AK-05	59.8673	-159.2178	278	1.33	0.988	9.0137	0.1817	4.9512	0.9813	69110	1377	12.26 ± 0.24	LLNL-CAMS
14AK-06	59.8677	-159.2180	267	1.41	0.988	9.8857	0.1803	5.6395	1.3862	71054	1758	12.76 ± 0.32	LLNL-CAMS
14AK-22	59.8693	-159.2188	229	2.71	0.988	11.4773	0.1821	5.9253	1.1879	65020	1325	12.25 ± 0.25	LLNL-CAMS
14AK-23	59.8692	-159.2185	237	1.23	0.988	11.1022	0.1826	5.5108	1.1246	62781	1287	11.58 ± 0.24	LLNL-CAMS
14AK-24	59.8690	-159.2184	244	1.57	0.988	12.0832	0.1828	6.0588	1.1719	63505	1233	11.66 ± 0.23	LLNL-CAMS
14AK-25	59.8688	-159.2184	239	1.73	0.988	17.5861	0.1823	7.1066	1.4606	50973	1059	*9.42 ± 0.20*	LLNL-CAMS
											Mean ± 1 S.D.	**12.09 ± 0.44 (0.49)**	
Inboard erratics													
14AK-26	59.8711	-159.2058	146	1.59	0.988	9.0775	0.1830	4.1506	0.8697	57906	1208	11.75 ± 0.25	LLNL-CAMS
14AK-27	59.8702	-159.2051	147	1.85	0.988	8.9614	0.1826	4.0453	1.0226	57038	1450	11.59 ± 0.30	LLNL-CAMS
14AK-31	59.8706	-159.2099	159	1.92	0.988	16.9613	0.1819	7.8131	1.4555	57991	1092	11.64 ± 0.22	LLNL-CAMS
											Mean ± 1 S.D.	**11.66 ± 0.08 (0.23)**	
Upvalley erratic													
14AK-28	59.8555	-159.2064	148	1.12	0.988	12.6558	0.1806	5.2278	1.2301	51514	1221	**10.39 ± 0.25 (0.31)**	LLNL-CAMS
Briner et al., 2002: ^{10}Be only													
M1													
MB1-99-1	59.8700	-159.2222	240	5	0.991	8.53	0.3739	2.3743	4.1517	70000	12000	11.97 ± 2.06	LLNL-CAMS
MB1-99-2	59.8707	-159.2235	236	5	0.993	12.80	0.3739	4.9411	5.1042	96400	10000	*16.58 ± 1.73*	LLNL-CAMS
MB1-99-3	59.8731	-159.2272	200	5	0.997	12.31	0.3739	4.7614	6.2517	96600	12700	*17.17 ± 2.27*	LLNL-CAMS
MB1-00-4	59.8676	-159.2196	287	5	0.991	32.14	0.5050	6.7351	3.3604	71000	4000	11.57 ± 0.65	LLNL-CAMS
M3													
MB6-00-1	59.8678	-159.2180	270	5	0.992	10.08	0.3550	2.6635	1.7941	63000	4000	10.44 ± 0.67	LLNL-CAMS
MB6-00-2	59.8683	-159.2183	273	5	0.992	25.38	0.4900	5.5951	2.0723	72000	3000	11.90 ± 0.50	LLNL-CAMS
equivalent moraine													
MB4-00-3	59.8703	-159.2706	274	5	0.997	20.56	0.3800	5.2894	4.1524	65000	5000	10.68 ± 0.82	LLNL-CAMS
											Mean ± 1 S.D. (n=5)	**11.31 ± 0.71 (0.74)**	

[a] Samples were spiked with LDEO carrier 5.1 with a ^{9}Be concentrations ranging from 1037.6 to 1039.1 ppm (see Table S2). Briner et al., 2002 samples were spiked with a 1000 ppm ^{9}Be carrier.

[b] All samples were measured at the Lawrence Livermore National Laboratory - Center for Accelerator Mass Spectrometry. Ratios are not corrected for ^{10}Be detected in procedural blanks.

[c] Concentrations are blank corrected by subtracting the total number of ^{10}Be atoms in the process blank; see Table S2 for process blank values.

Ages are calculated using version 3 of the exposure age calculator found at https://hess.ess.washington.edu/ (wrapper: 3.0, muons: 1A, consts: 3.0.3), which implements an updated treatment of muon-based production (Balco et al., 2008; Balco, 2017). All ages are calcualted using 'Lm' scaling and a Baffin Bay production rate of 4.04 ± 0.07 atoms g^{-1} yr^{-1}. (Young et al., 2013). This value has been updatd from the CRONUS v2 value of 3.96 ± 0.07 atoms g^{-1} yr^{-1}; the calibration dataset is the same. All samples assume zero erosion, use a density of 2.65 g cm^{-3}, standard air pressure 'std', and an effective attentuation length of 160 g cm^{-2}. ^{10}Be concentrations are reported relative to 07KNSTD with a reported ratio of 2.85 x 10^{-12} using a ^{10}Be half-life of 1.36 x 10^{6} years (Nishiizumi et al., 2007).

Numbers in parentheses are the moraine age uncertainties that include the uncertainty in the ^{10}Be production rate calibration dataset (1.8%). Briner et al., 2002 samples were measured relative to KNSTD.

We note that 14AK-09 and MB1-00-4 are replicate ^{10}Be measurements from the same M1 boulder, but different sample collections (see Fig. S2).

Table DR2. Process blank ^{10}Be data

Sample ID	Carrier added (g)	Carrier concentration[a]	$^{10}Be/^{9}Be$ ratio ± 1σ (10^{-16})	^{10}Be atoms	Samples applied to (Tables S1):
LDEO Carrier 5.1					
BLK1_2015Jan16	0.1810	1039.0	3.480 ± 0.886	*4375 ± 1116*	
BLK2_2015Jan16	0.1799	1039.0	2.540 ± 2.890	*3174 ± 3608*	
				3774 ± 849	14AK-04, -06, -15, -18, -28
BLK_2015Jan30	0.1805	1037.6	1.673 ± 1.964	***2094 ± 2458***	14AK-09, -10, -12, -17, -22, -25, -31
BLK_2015Jun12	0.1814	1039.1	1.528 ± 0.636	***1925 ± 801***	14AK-05, -16, -19, -23, -24, -26, -27

All ^{10}Be concentrations are reported relative to 07KNSTD with a reported ratio of 2.85×10^{-12} using a ^{10}Be half-life of 1.36×10^{6} years (Nishiizumi et al., 2007).

[a] evaporation-corrected carrier concentrations